



Contents lists available at ScienceDirect

Journal of the Taiwan Institute of Chemical Engineers

journal homepage: www.elsevier.com/locate/jtice

Low-cost sorbent for the removal of aniline and methyl orange from liquid-phase: Aloe Vera leaves wastes

Yusef Omid Khaniabadi^a, Rouhollah Heydari^b, Heshmatollah Nourmoradi^{c,d},
Hesam Basiri^e, Hassan Basiri^{f,*}

^a Health Care System of Karoon, Ahvaz Jundishapur University of Medical Sciences, Ahvaz, Iran

^b Razi Herbal Medicines Research Center, Lorestan University of Medical Sciences, P.O. Box 68149-89468, Khorramabad, Iran

^c Biotechnology and Medical Plants Research Center, Ilam University of Medical Sciences, Ilam, Iran

^d Department of Environmental Health Engineering, School of Health, Ilam University of Medical Sciences, Ilam, Iran

^e Department of Chemistry, Damghan Branch Islamic Azad University, Damghan, Iran

^f Department of Environmental Health Engineering, School of Health, Lorestan University of Medical Sciences, Khorramabad, Iran

ARTICLE INFO

Article history:

Received 17 June 2016

Revised 14 September 2016

Accepted 22 September 2016

Available online xxx

Keywords:

Adsorption

Aloe Vera leaves wastes

Aniline

Methyl orange

Kinetic

ABSTRACT

In this study, Aloe Vera leaves wastes-based sulfuric acid modified activated carbon (AV-SAC) was applied for the sorption of aniline as a health-toxic substance and methyl orange (MO) as a anionic dye from aqueous phase. The batch sorption system was used to assess the effect of different parameters including contact time, pH, adsorbent dosage, and adsorbate contents on the adsorption. The equilibrium was obtained at contact time of 60 min for both the adsorbates. The pH of 3 had a significant influence on the uptake capacities of aniline and MO from aqueous media. Fitting the experimental data to different kinetics and isotherms models indicated that the experimental data were well fitted by the pseudo-second-order kinetic and Freundlich isotherm models, respectively. The maximum monolayer adsorption capacities were acquired 185.18 and 196.07 mg/g for aniline and MO, respectively. Due to its low-cost and high uptake capacity, AV-SAC can be considered as one of the effective sorbents for wastewater treatment contains of aniline and MO.

© 2016 Taiwan Institute of Chemical Engineers. Published by Elsevier B.V. All rights reserved.

1. Introduction

Water pollution due to irregular discharge of many organic and inorganic pollutants by various industries wastewater is one of the most important environmental concerns in the current century, especially in the developing countries [1,2]. Aniline is one of the most important of these contaminants that widely found in wastewater from the pesticides, dyestuffs, paints, rubbers, pharmaceutical, and plastics industries [3–5]. It is very toxic and resistant to biodegradation compounds and also is harmful for human health [5–7]. U.S. Environmental Protection Agency (USEPA) has listed aniline as one of the priority contaminant [5]. Methyl orange (MO) or acid orange 52 is a water-soluble anionic dye that is widely used in textile, paper manufacturing, printing, food, and pharmaceutical industries [8]. It is regarded as an allergy-substance after contacting by skin, which causes shin eczema. Therefore, because of its toxic structure, its removal from aqueous media is very important [9]. Many treatment techniques in-

cluding photodecomposition, ion-exchange, electrolysis, membrane processes, photocatalyst, oxidation, biodegradation, and adsorption have been performed for the treatment of these compounds from polluted waters. Among these approaches, adsorption is an effective method due to its high efficiency, simplicity, and flexibility [10–12]. In general, adsorption is known as one of the best techniques for the separation and remove of various organic and inorganic impurities from wastewater [13,14]. This method do not generate harmful by-products and it is possible to regeneration of both the adsorbent and adsorbate [15,16]. One challenge faced by sorption technologies is the finding new adsorbents that effectively remove the organo-pollutants [3,17]. Due to high sorption capacity and high surface area, adsorption on the surface of activated carbon is generally used for the removal of toxic contaminants, but it is high-cost and difficult to regeneration [18,19]. Thus, several researches have been conducted for the production an activated carbon from available local agricultural wastes which are cheaper and have eco-friendly properties [20]. In addition to activated carbon, application of some non-conventional sorbents like lignin [3], graphitic carbon nitride [10], pine sawdust [21], Cr-bentonite [22], grafted acrylic acid [23], spherical carbon [24], organo-clay [25], Fe₃O₄-activated carbon [26], Moroccan clays [27], LDHs [28], tree

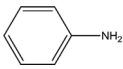
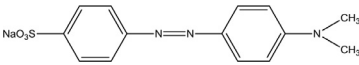
* Corresponding author. Fax: +98 6633412309.

E-mail address: h.basiri29@gmail.com (H. Basiri).

<http://dx.doi.org/10.1016/j.jtice.2016.09.025>

1876-1070/© 2016 Taiwan Institute of Chemical Engineers. Published by Elsevier B.V. All rights reserved.

Table 1
General characteristics and chemical structures of aniline and methyl orange.

Generic name	Scientific name	Chemical formula	Chemical structure	M_W (g/mol)	λ_{max} (nm)
Aniline	Aminobenzene	$C_6H_5NH_2$		93.13	260
Methyl orange	Acid orange 52	$C_{14}H_{14}N_3NaO_3S$		327.23	415

bark powder [29], metal-organic frameworks [9], chitosan [12], bottom ash [30], surfactant modified montmorillonite [31], etc. have been evaluated for the removal of aniline and MO from aqueous solutions. Aloe Vera is a tropical plant that widely grows in the warm areas such as United State, India, Australia, Africa, Mexico, South America, and Iran. The Aloe Vera leaves wastes are by-products of the agricultural and pharmaceutical industries that are applied to produce latex and drug substances [2]. In this work, activated carbon prepared from the Aloe Vera leaves wastes was modified by sulfuric acid and then used as a low-cost adsorbent for the sorption of aniline and MO from synthesized wastewater. The influences of various factors including contact time, pH, sorbent dosage and initial concentration of pollutants were evaluated and optimized on the adsorption.

2. Materials and methods

2.1. Materials

Aloe Vera leaves wastes were collected from suburban farms of Dezful and Ahvaz (cities of Khuzestan Province, Iran). The chemical substances including aniline (with purity greater than 99.5%), methyl orange, sulfuric acid and sodium hydroxide were purchased from Merck Co (Germany). Table 1 shows the characteristics and chemical structures of aniline and MO. The pH of solutions was adjusted with diluted and concentrated sulfuric acid and sodium hydroxide solutions using a digital pH-meter (50-pp-sartorius model). The stock solutions of aniline and MO (1000 mg/l) were prepared in distilled water and the working concentrations were also obtained with dilution of the stock solutions. The suspensions containing adsorbent and adsorbate were mixed using an orbital shaker (Behdad-Rotomix model, Iran) at 200 rpm.

2.2. Preparation of adsorbent

After separation the gel of Aloe Vera leaves, the remaining waste was carefully washed with deionized water to remove impurities and dried in an electrical oven at 150 °C for 24 h. Then, the dried leaves waste was crushed by a laboratory mill to obtain the particle size in the range of 300–600 μm. After that, particles were carbonized in a furnace at 550 °C for 20 min. The carbonized sample was transferred into 500 ml sulfuric acid solution (0.1 N) for 12 h. The suspension was filtered and the modified samples were washed several times with deionized water. Finally, the modified activated carbon was dried in an electrical oven at 105 °C for 12 h. The modified activated carbon-based Aloe Vera leaves waste (AV-SAC) was crushed and then sieved to have a uniform particle size of 40-mesh for the adsorption experiments.

2.3. Characterizations and analysis

The surface morphology of original and modified activated carbon, before and after the sorption process, was performed and characterized under a vacuum running by a scanning electron microscope (SEM, Jeol Model Jsm-T330) equipped through energy

dispersive X-ray Spectroscopy (EDX) system. Elemental analysis of Aloe Vera leaves wastes-based modified activated carbon (AV-SAC) was performed using a Heraeus Elemental Analyzer (Jobin-Yvon Ultima ICP-AES). FTIR spectra study of the original and modified activated carbon were also recorded by a FTIR spectrophotometer (JASCO, FT/IR-6300 Japan) with Diffuse Reflectance Technique (DRIFT) at resolution of 1 cm⁻¹ in the region of 400–4000 cm⁻¹. The concentrations of aniline and MO in the solution phases were determined by an UV-vis spectrophotometer (PG Instrument Limited Model, UK) at maximum wavelengths of 260 nm and 415 nm, respectively.

2.4. Determination of pH_{ZPC}

The pH at the zero point charge (pH_{ZPC}) for the Aloe Vera leaves waste-based activated carbon (AV-AC) and the sulfuric acid-modified activated carbon (AV-SAC) was determined by preparation 50 ml of 0.01 M NaCl solution into a series of 100 ml Erlenmeyer flasks. The initial pH values of NaCl solution were adjusted, as initial pH (pH_i), between 2 and 12 by adding H₂SO₄ (0.1 M) and NaOH (0.1 M) solutions. Then, sufficient amounts of adsorbent were poured into each flask and the suspensions were mixed by a mechanical shaker for 24 h at 200 rpm. After this period, the solutions pH was measured as finally pH (pH_f). The pH_{ZPC} was determined by plotting difference between pH_f and pH_i values (pH_{ZPC} = pH_f - pH_i) versus pH_i. The resulting curve with abscissa gives the pH_{ZPC}, the point at where pH is equal to zero.

2.5. Batch adsorption study

The batch sorption system was used to identify the influence of different parameters including contact time (0–90 min), pH (3–11), adsorbent dosage (1–5 g/l), and initial content of pollutants (20–100 mg/l) on the sorption of aniline and MO from synthesized wastewater. All of the adsorption experiments were carried out at room temperature (25 °C) and agitated in 200 rpm with 100 ml pollutant solution in 250 ml Erlenmeyer flasks. After the process, the mixture of adsorbates and AV-SAC was filtered using fiberglass paper. The sorption experiments were conducted in duplicates and the average amounts were considered. The uptake capacities of the sorbent were computed by Eq. (1):

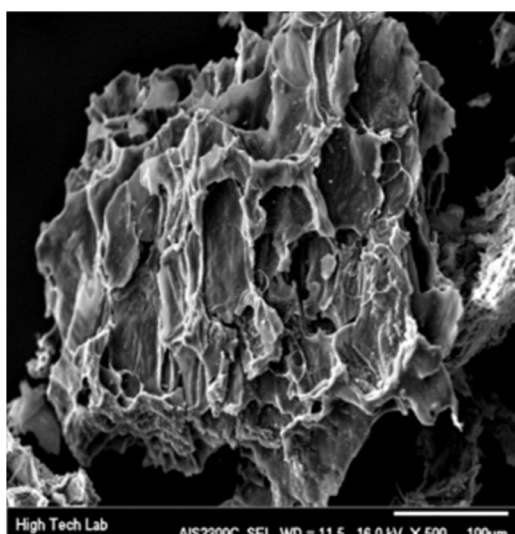
$$q_e = \frac{(C_0 - C_e)V}{m} \quad (1)$$

Where, q_e (mg/g) is the equilibrium uptake capacity of the adsorbates per gram AV-SAC. The parameters of C_0 and C_e (mg/l) are the initial and equilibrium concentrations of the pollutants, respectively. Also, V (l) is the volume of the solution and m (g) is the adsorbent mass [2].

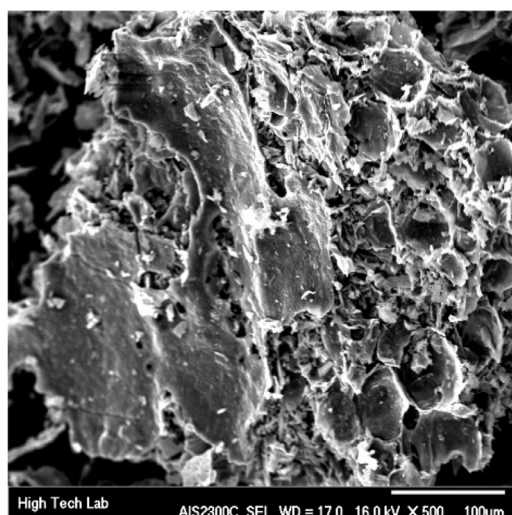
3. Results and discussion

3.1. Characterization

Fig. 1(a) and (b) show the surface morphology of the sorbent. As it is obvious from Fig. 1(a), the original activated carbon has



(a)

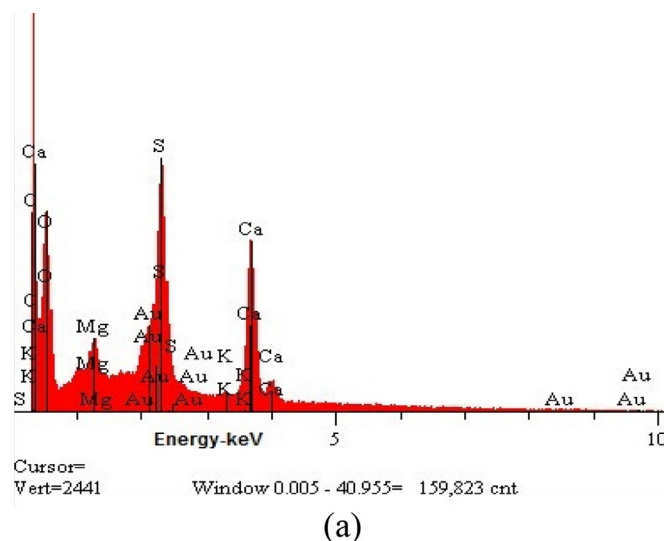


(b)

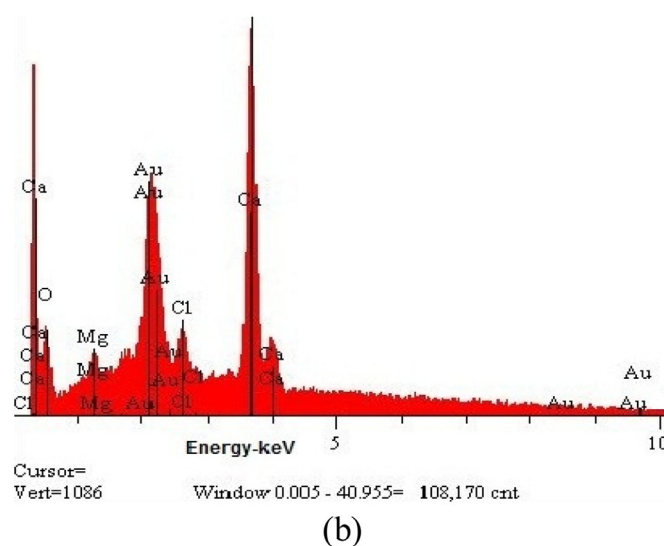
Fig. 1. SEM images of the sorbent ((a) before modification and (b) after modification).

cavities with more irregular, fine open pores, uneven structure and a relatively uniform pore size distribution. A regular structure for the modified activated carbon is shown in Fig. 1(b). In comparison with Fig. 1(a), highly regular pores are seen in Fig. 1(b), which shows a smoother surface and higher surface area. Highly regular pores can be in relation to the sulfuric acid as an effective activator in the developing pores of the AV-AC. Regular porous structure of the AV-SAC provided a higher surface area and subsequently the more active sites in the sorbent surface.

Chemical composition analysis of AV-AC shows that atoms including O, Ca, K and Mg are the main elements (92.7% of the total weight (wt%) of the sorbent. Other minor elements were involved Na (5.92%) and Cl (1.35%) [2,5]. Fig. 2(a) and (b) illustrate the SEM-EDX spectra of the sorbent before and after modification by sulfuric acid, respectively. As it can be seen, the original activated carbon was possessed with high concentrations of oxygen (43.82%) and sulfur (24.07%), and low concentrations of calcium (27.98%) and manganese (3.66%). A significant decrease in weight percentage of oxygen (28.30%) and sulfur (17.9%), and an increase in weight percentage of calcium (29.82%) and manganese (13.18%)



(a)



(b)

Fig. 2. SEM-EDX analytical results of (a) before and (b) after modification.

due to the modification by sulfuric acid were observed. The FTIR spectra of the AV-SAC before and after the sorption are illustrated in Fig. 3(a) and (b). Before the sorption, for AV-SAC, the IR bonds at around of 478, 622, and 1156 cm^{-1} were attributed to the stretching vibration of Si-O-Si, Si-O-M (M=Al or Mg), and Si-O groups, respectively. The characteristic bands at 1617 cm^{-1} is corresponding to water molecules bounded to light metals of Al and Mg. The low peak at 3237 cm^{-1} illustrated the O-H stretching vibration. After the uptake process (see Fig. 3(b)), the essential characteristic peaks at the regions of 3416 to 3552 cm^{-1} , which can be associated with interlayer water molecules stretching vibration, were shifted due to the uptake of pollutants onto the AV-SAC surface.

3.2. Effect of contact time

The influence of different contact times (0–90 min) on the sorption of aniline and MO by AV-SAC in 100 ml solution (50 mg/l for aniline and 100 mg/l for MO) and 2 g/l adsorbent was evaluated and the results are shown in Fig. 4(a). It is obvious that the adsorption capacities (q_e) for aniline and MO were quickly increased over the first 60 min and then slowly increased up to 90 min. This phenomenon can be due to the availability of a large number of positively charged free sites on the adsorbent surface

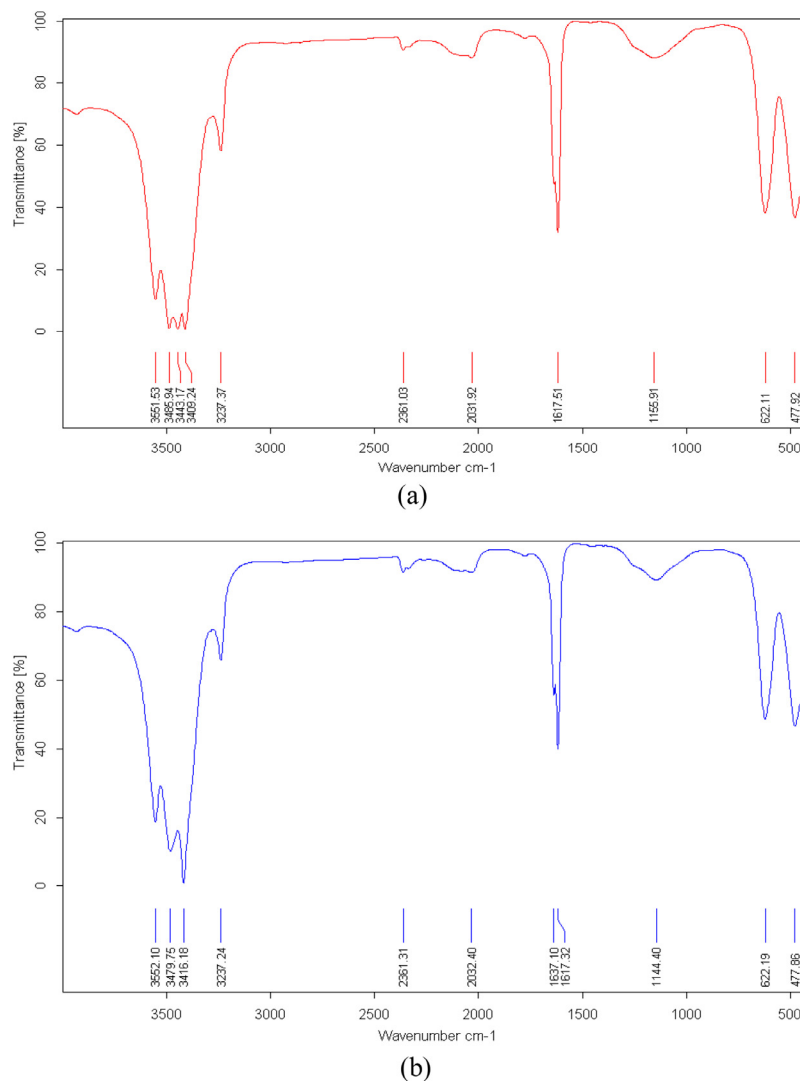


Fig. 3. FTIR spectra of AV-SAC (a) before and (b) after the sorption.

at the beginning of the process. As the time goes forward, the remaining free surface sites are difficult to be occupied because of the repulsive forces between the adsorbed pollutants and the pollutants in the liquid phase [24,32]. The sorption capacities of AV-SAC for aniline and MO at the equilibrium time were obtained 7.62 and 36.02 mg/g, respectively. Therefore, 60 min was selected as the optimum contact time for both the adsorbates in the subsequent experiments.

Hu et al. indicated that the equilibrium time for the uptake of aniline by graphitic carbon nitride was achieved during 24 h [10]. Lin et al. reported that the sorption of aniline by lignin grafted acrylic acid reached to equilibrium in the contact time of 60 min [23]. Al-Johani and Salam showed that aniline adsorption by multi-walled carbon nanotubes from liquid medium reached to equilibrium at contact time of 3 h [3]. Zaghouane-Boudiaf et al. obtained the equilibrium time equal to 40 min for the removal of MO by LDHs at an initial dye concentration of 50 mg/l [28]. Umpuch and Sakaew reported that the equilibrium was achieved after contact time of 60 min for the removal of MO by chitosan intercalated montmorillonite [33].

3.2.1. Kinetics study

The sorption kinetic data are needed for the selection of the optimum operating conditions in full-scale process [27,34]. For

this purpose, the experimental data were analyzed by various kinetic models including pseudo-first-order, pseudo-second-order, and intra-particle diffusion. The pseudo-first-order kinetic model can be illustrated by Eq. (2):

$$\ln(q_e - q_t) = \ln q_e - k_1 t \quad (2)$$

Where, q_e (mg/g) and q_t (mg/g) are the quantities of aniline and MO adsorbed onto the AV-SAC at the equilibrium and a particular time, respectively. K_1 (1/min) is the rate constant of the pseudo-first-order kinetic model. K_1 and q_e were acquired from the slope and intercept of linear plotting $\ln(q_e - q_t)$ versus t , respectively. The values of calculated q_e , K_1 and correlation coefficient (R^2) are shown in Table 2. The experimental data were also studied by pseudo-second-order kinetic model. A pseudo-second-order kinetic equation is given as Eq. (3) [35,36]:

$$\frac{t}{q_t} = \frac{1}{k_2 q_e^2} + \frac{t}{q_e} \quad (3)$$

Where, q_e and q_t (mg/g) are the parameters that were defined above to the pseudo-first-order kinetic model. K_2 (g/mg min) is the rate constant of the pseudo-second-order model. As shown in Fig. 4(b), K_2 and q_e were acquired from the intercept and slope of plotting t/q_t versus t , respectively.

Table 2

Parameters of pseudo-first-order and pseudo-second-order models in present study.

Adsorbate	Pseudo-first-order			Pseudo-second-order			Intra-particle diffusion			
	q_e , experimental (mg/g)	K_1 (1/min)	R^2	q_e , experimental (mg/g)	q_e , calculated (mg/g)	K_2 (g/mg.min)	R^2	K (mg/g min ^{1/2})	C (mg/g)	R^2
Aniline	2.13	0.017	0.96	7.62	9.34	0.011	0.99	0.561	2.99	0.91
MO	1.65	0.014	0.64	36.02	40	0.0055	0.99	0.631	30.98	0.88

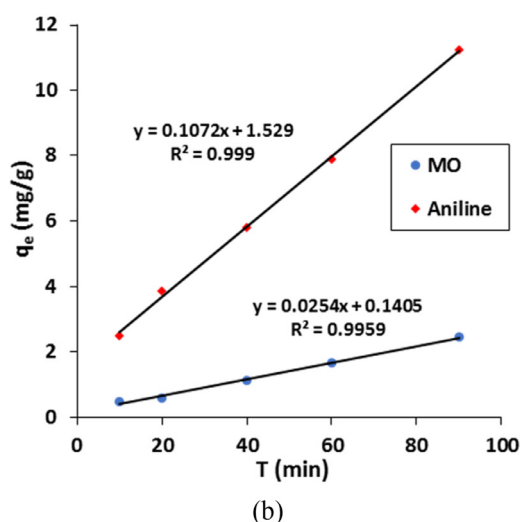
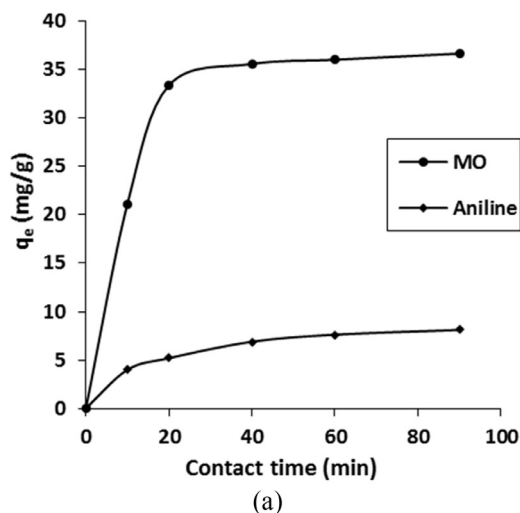


Fig. 4. (a) Effect of contact time on the sorption capacity (aniline concentration = 50 mg/l, MO concentration = 100 mg/l, adsorption dosage = 2 g/l at pH = 7) and (b) pseudo-second-order kinetic model.

The intra-particle diffusion model can be expressed by the following equation:

$$q_t = k_{id}t^{1/2} + C_i \quad (4)$$

Where, k_{id} is the rate constant of the intra-particle diffusion model (mg/g min^{1/2}), q_t (mg/g) is the adsorbate uptake at time t (min) and C_i (mg/g) is the thickness of the boundary layer. The values of k_{id} and C_i were estimated from the slope and intercept of the liner regression of the plot of q_t versus $t^{1/2}$, respectively. Table 2 presents the values of the intra-particle diffusion kinetic model parameters. As listed, the amounts of C for the sorption of MO and aniline with the sorbent were 30.98 mg/g and 2.99 mg/g, respectively. These values demonstrated that the regression line of this model did not pass from the zero point (figure not shown).

Therefore, it can be concluded that the intra-particle diffusion is not the solely rate-limiting step in the sorption process.

The values of correlation coefficient of the kinetics models are also shown in Table 2. As can be seen, the amounts of the correlation coefficient for pseudo-second-order model were more than of pseudo-first-order kinetic and intra-particle diffusion models. Therefore, the adsorption process of aniline and MO by AV-SAC followed from the pseudo-second-order kinetic model. Similar kinetic results were reported for the uptake of aniline onto other adsorbents such as multi-walled carbon nanotubes [3], graphitic carbon nitride [10], oxygen plasma irradiated bamboo based activated carbon [37], and Fe₃O₄ activated carbon magnetic nanoparticles [26]. Zhang et al. reported that the sorption of aniline by L-g-AA from synthetic wastewater was well described by pseudo-second-order kinetic model [22]. Experimental data of the sorption of MO using Kaolinite [38], chitosan intercalated montmorillonite [33], Prosopis juliflora [39], and HJ-P01 resin [40] were fitted by pseudo-second-order kinetic model. Qiu et al. presented that the experimental data for sorption of the MO onto RH-AC were well fitted by pseudo-second-order kinetic model [41].

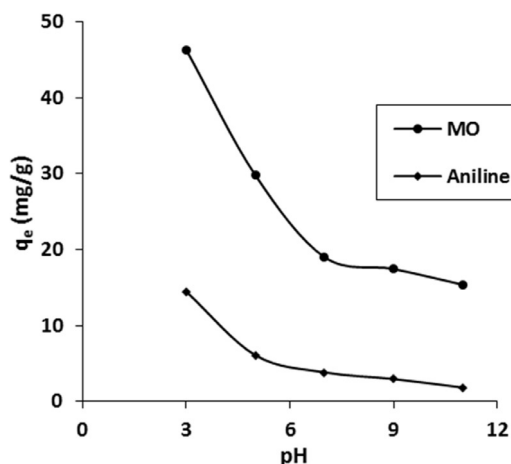
3.3. Effect of pH and determination of zero point charge

The solution pH changes the surface properties of sorbent and also the degree of ionization of adsorbates [42]. The effect of solution pH (3–11) on the adsorption of aniline and MO by AV-SAC from aqueous solution is shown in Fig. 5(a). As can be seen, the sorption capacities of the aniline and MO were reduced with increase the solution pH from 3 to 11. The maximum sorption capacities of aniline and MO with amounts of 14.47 and 46.31 mg/g were occurred at pH 3, respectively. These results may be due to change in the surface charges of the sorbent. The positive charges of the adsorbent surface were increased with decrease the solution pH, which this led to increase the sorption capacity of the sorbent in acidic solution pH [43,44]. Thus, pH 3 was chosen as the optimum for the subsequent stages.

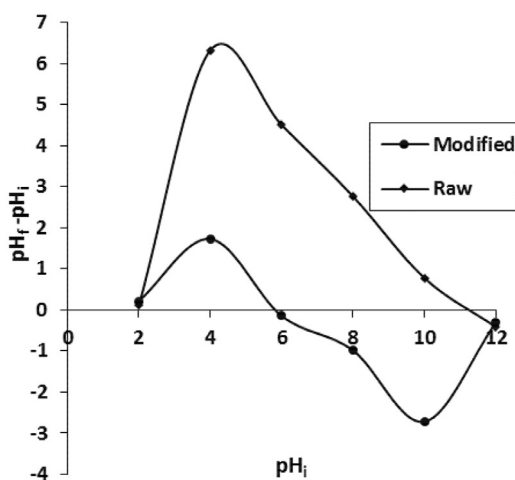
To understand the sorption mechanism, it is required to determine the zero point charge (pH_{zpc}) of the adsorbent [45]. On the other hand, pH_{zpc} is a very important parameter to identify the interaction of sorbent surface with adsorbate [46,47]. It has been identified that at any pH below pH_{zpc}, the surface charge is positive, whereas at pH higher than pH_{zpc}, the surface charge is negative [23]. Fig. 5(b) shows the pH_{zpc} of the Aloe Vera leaves wastes-based activated carbon before and after modification by sulfuric acid. As it is obvious, the pH_{zpc} of original and AV-SAC were found to be equal 11.3 and 5.8, respectively. Regarding pH_{zpc}, it can be stated that the surface of the activated carbon is de-protonated at pH values higher than 11.3 and 5.8 for AV-AC and AV-SAC, respectively. Hence, the sorption of negatively charged of aniline and MO was hindered at pH values above pH_{zpc}.

3.4. Effect of adsorbent dosage

The effect of adsorbent dosage (1–5 g/l) on the sorption capacities of aniline and MO by AV-SAC is illustrated in Fig. 6. As seen, the sorption capacities of the aniline and MO were quickly decreased from 33.7 and 72.49 mg/g to 5.62 and 9.8 mg/g with



(a)



(b)

Fig. 5. (a) Effect of pH on the sorption capacity (contact time = 60 min, aniline concentration = 50 mg/l, MO concentration = 100 mg/l, and adsorption dosage = 2 g/l) and (b) pHZpc of the sorbent.

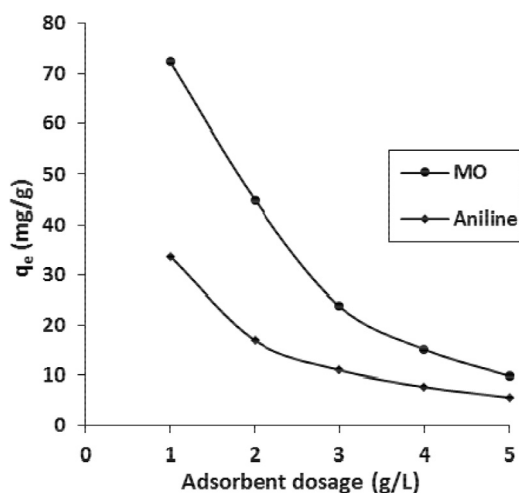
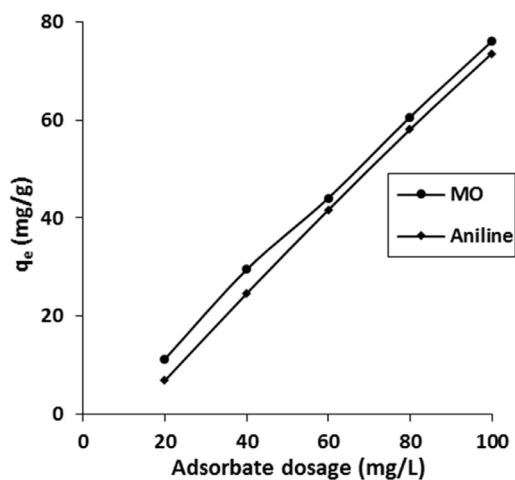
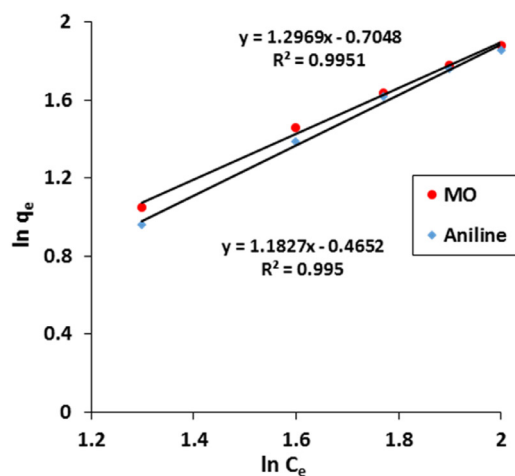


Fig. 6. Effect of adsorbent dosage on the sorption capacity (contact time = 60 min, aniline concentration = 50 mg/l, MO concentration = 100 mg/l, and solution pH = 3).



(a)



(b)

Fig. 7. (a) Effect of initial concentration on the sorption capacity (contact time = 60 min, adsorbent dosage = 1 g/l, and solution pH = 3) and (b) Freundlich isotherm model.

increase the adsorbent dosage from 1 to 5 g/l, respectively. Decreasing the sorption rate of aniline and MO in the higher dosages of AV-SAC can be due to the less availability of the sorbent active sites resulted from gathering and overlapping the adsorbent particles. Therefore, the adsorbent dosage of 1 g/l was selected as the optimum dosage for the next experiments.

3.5. Effect of initial adsorbate concentration

The effect of various initial adsorbate concentrations (20–100 mg/l) was investigated on the sorption of aniline and MO in contact time of 60 min, adsorbent dosage of 1 g/l, and pH 3 at room temperature (25 °C). The results of initial adsorbate concentration on the sorption are presented in Fig. 7(a). As shown, with increasing the initial concentration of pollutants from 20 to 100 mg/l, the sorbent capacities of the sorbent for aniline and MO were gradually increased. This probably due to increase in driving force of aniline and MO molecules including Vander Waal's force to the surface active sites of the adsorbent that happens at the higher concentrations of the adsorbates.

3.5.1. Isotherm study

The adsorption isotherms are useful parameters to find out the adsorbate distribution in the liquid phase onto the solid phase in

Table 3
Parameters of Langmuir and Freundlich isotherm models obtained from this study.

Adsorbate	Langmuir isotherm			Freundlich isotherm			D-R isotherm			
	Q_m (mg/g)	b (l/g)	R^2	R_L	K_f (l/g)	n	R^2	q_m (mg/g)	E (kJ/mol)	R^2
Aniline	185.18	0.003	0.91	0.86	0.33	0.85	0.99	187.53	0.072	0.96
MO	196.07	0.002	0.69	0.83	0.15	0.77	0.99	95.20	0.133	0.95

Table 4
The comparison of adsorption capacities of aniline and MO by various adsorbents.

Adsorbent	Adsorbate	Equilibrium time (min)	Conc. (mg/l)	pH	Max. adsorption capacity (mg/g)	Ref.
Pine sawdust	Aniline	80	30	6.2	1.5	[56]
Activated carbon/chitosan composite	Aniline	120	50	7	22.90	[57]
PAM/SiO ₂	Aniline	300	1000	8	52.0	[6]
Fe ₃ O ₄ -activated carbon magnetic nanoparticles	Aniline	300	300	6	90.91	[26]
Graphitic carbon nitride	Aniline	1200	30	4	71.9	[10]
Spherical carbon	Aniline	10	40	6.5	93.59	[24]
Bamboo based activated carbon	Aniline	450	300	7	104.17	[13]
Aloe Vera-activated carbon	Aniline	60	100	3	106.38	[5]
Lignin grafted acrylic acid	Aniline	90	500	7	127.06	[23]
AV-SAC	Aniline	60	100	3	185.18	This study
Kaolinite	MO	15	20	2.5	1.24	[38]
Rice husk	MO	25	35	2	1.29	[58]
Egussi peeling	MO	25	35	2	13.88	[58]
Na-MMT	MO	60	550	3	24.0	[31]
γ -Fe ₂ O ₃ /chitosan composite films	MO	–	60	3	29.41	[12]
Chitosan	MO	–	100	4	34.83	[59]
MgNiAl-CO ₃	MO	100	100	8	118.5	[28]
CTS/MMT	MO	60	200	2	123.46	[33]
Zn/Al-LDO	MO	–	100	6	181.9	[60]
AV-SAC	MO	60	100	3	196.07	This study

the equilibrium state [42,48,49]. Hence, three isotherms including Langmuir, Freundlich and Dubinin–Radushkevich (D–R) isotherm models were investigated for this study. The Langmuir isotherm approximates the greatest monolayer sorption on the uniform surface of the solid phase [35,50,51]. The linearized form of Langmuir isotherm is reported by the Eq. (5):

$$\frac{C_e}{q_e} = \frac{C_e}{Q_m} + \frac{1}{bQ_m} \quad (5)$$

Where, C_e (mg/l) and q_e (mg/g) were the initial concentration of adsorbate and the sorption capacity of adsorbent in the equilibrium time, respectively. Q_m (mg/g) is the maximum uptake capacity and b (l/mg) is the Langmuir rate constant. Q_m and b are acquired from the slope and intercept of linear plotting C_e/q_e against C_e , respectively [51,52].

The Langmuir isotherm is shown by a dimensionless constant separation factor (R_L). This factor also called the equilibrium factor, which is computed using the following equation [48]:

$$R_L = \frac{1}{1 + bC_0} \quad (6)$$

Where, C_0 is the initial concentrations of aniline and MO. The value of separation factor (R_L) shows the adsorption condition as unfavorable (R_L more than 1), liner (R_L equals to 1), irreversible (R_L equals to 0), and favorable (R_L between 0 and 1). According to the values of R_L ($R_L=0.86$ and 0.83 for aniline and MO, respectively), the adsorption process of two adsorbates by AV-SAC was favorable. The amounts of Q_m , b , R^2 and R_L for both adsorbates are listed in Table 3.

Freundlich isotherm model is typically described for multilayer sorption onto a heterogeneous solid surface [53]. This isotherm is shown by Eq. (7):

$$\ln q_e = \ln k_f + \frac{1}{n} \ln C_e \quad (7)$$

Where, K_f (l/g) and n are the Freundlich constants and show the capacity and intensity of the sorption process, respectively [54]. As demonstrated in Fig. 7(b), K_f and n were determined by the intercept and slope of plotting $\ln q_e$ against $\ln C_e$, respectively [51].

Dubinin–Radushkevich (D–R) isotherm has been used to determine the physical or chemical nature of adsorption process [24,32]. The D–R isotherm can be illustrated by Eq. (8):

$$\ln q_e = \ln q_m - \beta \varepsilon^2 \quad (8)$$

Where, q_m (mg/g) is the theoretical adsorption capacity at saturation state, β and ε are the constant related to uptake energy and Polanyi potential, respectively. q_m and β are acquired from the intercept and the slope of liner plot of $\ln q_e$ versus ε^2 , respectively. ε is also obtained from the Eq. (9):

$$\varepsilon = RT \ln \left(1 + \frac{1}{C_e} \right) \quad (9)$$

Where, R and T are the universal gas constant (8.3 kJ/mol K) and the solution temperature (°K), respectively. The mean uptake energy, E (kJ/mol), is determined by Eq. (10):

$$E = \frac{1}{\sqrt{2\beta}} \quad (10)$$

In D–R isotherm, the E value shows the sorption type. When $E < 8$ kJ/mol, 8–16 kJ/mol and $E > 16$ kJ/mol, the physical adsorption, chemical ion exchange and chemical adsorption are occurred, respectively [24,32]. As presented in Table 3, the E values of 0.13 and 0.07 kJ/mol were acquired for the sorption of aniline and MO by the adsorbent, respectively. Therefore, it can be concluded that the adsorption of both the adsorbates by the sorbent was physical in nature.

As it can be seen in Table 3, Freundlich isotherm model had higher R^2 value than Langmuir isotherm model. Therefore, the sorption data of aniline and MO onto AV-SAC were well fitted by the Freundlich isotherm model. Zhang and Li demonstrated that

experimental data the sorption of aniline via Hypercross-Linked Fiber was fitted by Freundlich isotherm model [55]. Fumba et al. illustrated that the sorption of MO onto the activated geopolymer was well followed from Freundlich isotherm model [38].

3.6. Comparison with other studies

Table 4 illustrates the comparison of adsorption capacities of various adsorbents for aniline and MO from liquid media. As shown, the maximum uptake capacity (Q_m , mg/g) of activated carbon synthesized from Aloe Vera leaves wastes in comparison with other types of sorbents had a higher sorption capacity. Thus, this adsorbent is an effective option for the removal of aniline and MO from aqueous phase.

4. Conclusion

In this research, Aloe Vera leaves wastes-based activated carbon was modified by sulfuric acid (AV-SAC) and then used as a cheap adsorbent for the sorption of aniline and methyl orange (MO) from aqueous media. Influential parameters such as contact time, pH, adsorbent dosage, and initial concentration of aniline and MO were evaluated on the sorption process. The equilibrium for both the adsorbates was obtained at the contact time of 60 min. The acidic pH had a significant effect on the sorption of aniline and MO. The uptake of aniline and MO onto the AV-SAC surface was well described by the pseudo-second-order kinetic and Freundlich isotherm models. The results showed that this natural adsorbent has advantages including low-cost, eco-friendly, high-sorption capacity and non-toxicity. Therefore, it can be considered as an effective sorbent on the uptake of aniline and MO from aqueous solution.

Acknowledgments

The authors wish to thank Vice Chancellery for Research of Lorestan University of Medical Sciences for financial supporting this study.

References

- [1] Dong K, Qiu F, Guo X, Xu J, Yang D, He K. Adsorption behavior of azo dye eriochrome black-T from aqueous solution by β -cyclodextrins/polyurethane foam. *Mater Polym Plast Technol Eng* 2013;52:452–60.
- [2] Omidi-Khaniabadi Y, Jafari A, Nourmoradi H, Taheri F, Saeedi S. Adsorption of 4-chlorophenol from aqueous solution using activated carbon synthesized from aloe vera green wastes. *J Adv Environ Health Res* 2015;3(2):120–9.
- [3] Al-Johani H, Salam MA. Kinetics and thermodynamic study of aniline adsorption by multi-walled carbon nanotubes from aqueous solution. *J Colloid Interface Sci* 2011;360:760–7.
- [4] Dvořák L, Lederer T, Jirku V, Masák J, Novák L. Removal of aniline, cyanides and diphenylguanidine from industrial wastewater using a full-scale moving bed biofilm reactor. *Process Biochem* 2014;49:102–9.
- [5] Basiri H, Nourmoradi H, Moghadam FM, Moghadam KF, Mohammadian J, Khaniabadi YO. Removal of aniline as a health-toxic substance from polluted water by aloe vera waste-based activated carbon. *Der Pharma Chem* 2015;7(11):149–55.
- [6] An F, Feng X, Gao B. Adsorption of aniline from aqueous solution using novel adsorbent PAM/SiO₂. *Chem Eng J* 2009;151:183–7.
- [7] Yu S, Wang X, Ai Y, Tan X, Hayat T, Hu W, et al. Experimental and theoretical studies on competitive adsorption of aromatic compounds on reduced graphene oxides. *J Mater Chem A* 2016;4:5654–62.
- [8] Chen Z-X, Jin X-Y, Chen Z, Megharaj M, Naidu R. Removal of methyl orange from aqueous solution using bentonite-supported nanoscale zero-valent iron. *J Colloid Interface Sci* 2011;363:601–7.
- [9] Haque E, Lee JE, Jang IT, Hwang YK, Chang J-S, Jegal J, et al. Adsorptive removal of methyl orange from aqueous solution with metal-organic frameworks, porous chromium-benzenedicarboxylates. *J Hazard Mater* 2010;181:535–42.
- [10] Hu R, Wang X, Dai S, Shao D, Hayat T, Alsaedi A. Application of graphitic carbon nitride for the removal of Pb(II) and aniline from aqueous solutions. *Chem Eng J* 2015;260:469–77.
- [11] Ahmed MJ, Theydan SK. Adsorption of p-chlorophenol onto microporous activated carbon from Albizia lebbek seed pods by one-step microwave assisted activation. *J Anal Appl Pyrolysis* 2013;100:253–60.
- [12] Jiang R, Fu Y-Q, Zhu H-Y, Yao J, Xiao L. Removal of methyl orange from aqueous solutions by magnetic maghemite/chitosan nanocomposite films: Adsorption kinetics and equilibrium. *J Appl Polym Sci* 2012;125:540–9.
- [13] Wua G, Zhang X, Hui H, Yan J, Zhang Q, Wan J, et al. Adsorptive removal of aniline from aqueous solution by oxygen plasma irradiated bamboo based activated carbon. *Chem Eng J* 2012;185–186:201–10.
- [14] Ladhe U, Wankhede S, Patil V, Patil P. Adsorption of Eriochrome black T from aqueous solutions on activated carbon prepared from mosambi peel. *J Appl Sci Environ Sanit* 2011;6(2):149–54.
- [15] Laszlo K. Adsorption from aqueous phenol and aniline solutions on activated carbons with different surface chemistry. *Colloids Surf A* 2005;265:32–9.
- [16] Monsalvo V, Mohedano A, Rodriguez J. Activated carbons from sewage sludge application to aqueous-phase adsorption of 4-chlorophenol. *Desalination* 2011;277:377–82.
- [17] Omidi Y, Kamareei B, Nourmoradi H, Basiri H, Heidari S. Hexadecyl trimethyl ammonium bromide-modified montmorillonite as a low-cost sorbent for the removal of methyl red from liquid-medium. *IJE Trans A Basics* 2016;29(1):60–7.
- [18] Zhanga B, Lia F, Wub T, Sunb D, Lia Y. Adsorption of p-nitrophenol from aqueous solutions using nanographite. *Colloids Surf A Physicochem Eng Asp* 2015;464:78–88.
- [19] Yao T, Guo S, Zeng C, Wang C, Zhang L. Investigation on efficient adsorption of cationic dyes on porous magnetic polyacrylamide microspheres. *J Hazard Mater* 2015;292:90–7.
- [20] Luna MDGd, Flores ED, Genuino DAD, Futralan CM, Wan M-W. Adsorption of Eriochrome Black T (EBT) dye using activated carbon prepared from waste rice hulls-optimization, isotherm and kinetic studies. *J Taiwan Inst Chem Eng* 2013;44:646–53.
- [21] Zhou Y, Gu X, Zhang R, Lu I. Removal of aniline from aqueous solution using pine sawdust modified with citric acid and β -cyclodextrin. *Ind Eng Chem Res* 2014;53:887–94.
- [22] Zheng H, Liu D, Zheng Y, Liang S, Liu Z. Sorption isotherm and kinetic modeling of aniline on Cr-bentonite. *J Hazard Mater* 2009;167:141–7.
- [23] Lin X, Zhang J, Luo X, Zhang C, Zhou Y. Removal of aniline using lignin grafted acrylic acid from aqueous solution. *Chem Eng J* 2011;172:856–63.
- [24] Roshan B, Kadirvelu K, Kumar NS. Investigation of aniline adsorption onto spherical carbon: Optimization using response surface methodology. *Int J Eng Res Appl* 2013;3(5):943–52.
- [25] Kuo S-L, Wu EM-Y. Adsorption of cadmium and aniline of organoclay by HDTMA and CDTEA intercalating. *J Indian Chem Soc* 2014;91:1–7.
- [26] Kakavandi B, Jafari A, Kalantary R, Nasser S, Ameri A, Esrafilly A. Synthesis and properties of Fe₃O₄ activated carbon magnetic nanoparticles for removal of aniline from aqueous solution: equilibrium, kinetic and thermodynamic studies. *Iran J Environ Health Sci* 2013;10(19):2–9.
- [27] Elmoubarki R, Mahjoubi F, Tounsadi H, Moustadraf J, Abdennouri M, Zouhri A, et al. Adsorption of textile dyes on raw and decanted Moroccan clays: Kinetics, equilibrium and thermodynamics. *Water Resour India* 2015;9:16–29.
- [28] Zaghouane-Boudiaf H, Boutahala M, Arab L. Removal of methyl orange from aqueous solution by uncalcined and calcined MgNiAl layered double hydroxides (LDHs). *Chem Eng J* 2012;187:142–9.
- [29] Dim PE. Adsorption of methyl red and methyl orange using different tree bark powder. *Acad Res Int* 2013;4(1):330–8.
- [30] Mittal A, Malviy A, Kaur D, Mittal J, Kurup L. Studies on the adsorption kinetics and isotherms for the removal and recovery of methyl orange from wastewaters using waste materials. *J Hazard Mater* 2007;148:229–40.
- [31] Chen D, Chen J, Luan X, Ji H, Xia Z. Characterization of anion-cationic surfactants modified montmorillonite and its application for the removal of methyl orange. *Chem Eng J* 2011;171:150–8.
- [32] Nourmoradi H, Avazpour M, Ghasemian N, Heidari M, Moradnejadi K, Khodarahmi F, et al. Surfactant modified montmorillonite as a low cost adsorbent for 4-chlorophenol: Equilibrium, kinetic and thermodynamic study. *J Taiwan Inst Chem Eng* 2016;59:244–51.
- [33] Umpuch C, Sakaew S. Removal of methyl orange from aqueous solutions by adsorption using chitosan intercalated montmorillonite. *Songklanakarin J Sci Technol* 2013;35(4):451–9.
- [34] Chatterjee S, Lee MW, Woo SH. Adsorption of congo red by chitosan hydrogel beads impregnated with carbon nanotubes. *Bioresour Technol* 2010;101:1800–6.
- [35] Liu Q, Yang B, Zhang L, Huang R. Adsorption of an anionic azo dye by cross-linked chitosan/bentonite composite. *Int J Biol Macromol* 2015;72:1129–35.
- [36] Chaari I, Feki M, Medhioub M, Bouzid J, Fakhfakh E, Jamoussi F. Adsorption of a textile dye "Indanthrene Blue RS (C.I. Vat Blue 4)" from aqueous solutions onto smectite-rich clayey rock. *J Hazard Mater* 2009;172:1623–8.
- [37] Wu G-Q, Zhang X, Hui H, Yan J, Zhang Q-S, Wan J-L, et al. Adsorptive removal of aniline from aqueous solution by oxygen plasma irradiated bamboo based activated carbon. *Chem Eng J* 2012;185–186:201–10.
- [38] Fumba G, Essomba JS, Tagne GM, Nsami JN, Béliibi PDB, Mbadcam JK. Equilibrium and kinetic adsorption studies of methyl orange from aqueous solutions using kaolinite, metakaolinite and activated geopolymer as low cost adsorbents. *J Acad Indus Res* 2014;3(4):156–63.
- [39] Kumar M, Tamilarasan R. Modeling of experimental data for the adsorption of methyl orange from aqueous solution using a low cost activated carbon prepared from Prosopis juliflora. *Pol J Chem Technol* 2013;15(2):29–39.
- [40] Huang J. Adsorption thermodynamics of methyl orange from aqueous solution onto a hyper-cross-linked polystyrene resin modified with phenolic hydroxy groups. *Adsorpt Sci Technol* 2010;28(5):397–405.

- [41] Qiu M, Xiong S, Wang G, Xu J, Luo P, Ren S, et al. Kinetic for adsorption of dye methyl orange by the modified activated carbon from rice husk. *Adv J Food Sci Technol* 2015;9(2):140–5.
- [42] Ghaedi M, Khajesharifi H, Yadhuri AH, Roosta M, Sahraei R, Daneshfar A. Cadmium hydroxide nanowire loaded on activated carbon as efficient adsorbent for removal of Bromocresol Green. *Spectrochim Acta Part A* 2012;86:62–8.
- [43] Jin Z, Wang X, Sun Y, Ai Y, Wang X. Adsorption of 4-n-nonylphenol and bisphenol-A on magnetic reduced graphene oxides: A combined experimental and theoretical studies. *Environ Sci Technol* 2015;49:9168–75.
- [44] Zhang S, Zeng M, Li J, Li J, Xub J, Wang X. Porous magnetic carbon sheets from biomass as an adsorbent for the fast removal of organic pollutants from aqueous solution. *J Mater Chem A* 2014;2:4391–7.
- [45] Wang L, Zhang J, Wang A. Removal of methylene blue from aqueous solution using chitosan-g-poly (acrylic acid)/montmorillonite superadsorbent nanocomposite. *Colloids Surf. A* 2008;322:47–53.
- [46] Cengiz S, Tanrikulu F, Aksu S. An alternative source of adsorbent for the removal of dyes from textile waters: *Posidonia oceanica* (L.). *Chem Eng J* 2012;189–190:32–40.
- [47] Zhao G, Jiang L, He Y, Li J, Dong H, Wang X, et al. Sulfonated graphene for persistent aromatic pollutant management. *Adv Mater* 2011;23(34):3959–63.
- [48] Almeida C, Debacher N, Downs A, Cottet L, Mello C. Removal of methylene blue from colored effluents by adsorption on montmorillonite clay. *J Colloid Interface Sci* 2009;332:46–53.
- [49] Chatterjee S, Lee MW, Woo SH. Adsorption of congo red by chitosan hydrogel beads impregnated with carbon nanotubes. *Bioresour Technol* 2010;101:1800–6.
- [50] Nourmoradi H, Nikaeen M, Khiadani M. Removal of benzene, toluene, ethylbenzene and xylene (BTEX) from aqueous solutions by montmorillonite modified with nonionic surfactant: Equilibrium, kinetic and thermodynamic study. *Chem Eng J* 2012;191:341–8.
- [51] Jourvand M, Khorramabadi GS, Omidi-Khaniabadi Y, Godini H, Nourmoradi H. Removal of methylene blue from aqueous solutions using modified clay. *J Bas Res Med Sci* 2015;2(1):32–41.
- [52] Wu FC, Wu PH, Tseng RL, Juang RS. Preparation of novel activated carbons from H₂SO₄ pretreated corncob hulls with KOH activation for quick adsorption of dye and 4-chlorophenol. *J Environ Manag* 2011;92:708–13.
- [53] Langmuir I. The adsorption of gases on plane surfaces of glass, mica and platinum. *J Am Chem Soc* 1918;40:1361–403.
- [54] Nourmoradi H, Ghiasvand A, Noorimotlagh Z. Removal of methylene blue and acid orange7 from aqueous solutions by activated carbon coated with zinc oxide (ZnO) nanoparticles: Equilibrium, kinetic and thermodynamic study. *Desalination Water Treat* 2015;55(1):252–62.
- [55] Zhang Y, Li D. Adsorption mechanism for aniline on the hypercross-linked fiber. *Iran J Chem Chem Eng* 2012;31(3):29–34.
- [56] Zhou Y, Gu X, Zhang R, Lu J. Removal of aniline from aqueous solution using pine sawdust modified with citric acid and β -cyclodextrin. *Ind Eng Chem Res* 2014;53:887–94.
- [57] Huang R, Yang B, Liu Q, Liu Y. Simultaneous adsorption of aniline and Cr (VI) ion by activated carbon/chitosan composite. *J Appl Polym Sci* 2014;131:39903.
- [58] Tchuifon D, Anagho S, Njanja E, Ghogomu J, Ndifor-angwafor N, Kamgaing T. Equilibrium and kinetic modeling of methyl orange adsorption from aqueous solution using rice husk and egussi peeling. *Int J Chem Sci* 2014;12(3):741–61.
- [59] Saha TK, Bhoumik NC, Karmaker S, Ahmed MG, Ichikawa H, Fukumori Y. Adsorption of methyl orange onto chitosan from aqueous solution. *J Water Resour Prot* 2010;2:898–906.
- [60] Ni Z-M, Xia S-J, Wang L-G, Xing F-F, Pan G-X. Treatment of methyl orange by calcined layered double hydroxides in aqueous solution: adsorption property and kinetic studies. *J Colloid Interface Sci* 2007;316:284–91.